Nutz, T., Androvitsaneas, P., Young, A., Oulton, R., & McCutcheon, D. P. S. (2019). Stabilization of an optical transition energy via nuclear Zeno dynamics in quantum-dot-cavity systems. *Physical Review A*, *99*(5), [053853]. https://doi.org/10.1103/PhysRevA.99.053853

Stabilization of an optical transition energy via nuclear Zeno dynamics in quantum-dot–cavity systems

Thomas Nutz,[1,2,*] Petros Androvitsaneas,[2] Andrew Young,[2] Ruth Oulton,[2] and Dara P. S. McCutcheon[2]
[1] *Controlled Quantum Dynamics Theory Group, Imperial College London, London SW7 2AZ, United Kingdom*
[2] *Quantum Engineering Technology Labs, H. H. Wills Physics Laboratory and Department of Electrical and Electronic Engineering, University of Bristol, Bristol BS8 1FD, United Kingdom*

(Received 15 January 2019; published 31 May 2019)

We investigate the effect of nuclear spins on the phase shift and polarization rotation of photons scattered off a quantum-dot–cavity system. We show that as the phase shift depends strongly on the resonance energy of an electronic transition in the quantum dot, it can provide a sensitive probe of the quantum state of nuclear spins that broaden this transition energy. By including the electron-nuclear spin coupling at a Hamiltonian level within an extended input-output formalism, we show how a photon-scattering event acts as a nuclear spin measurement, which when rapidly applied leads to an inhibition of the nuclear dynamics via the quantum Zeno effect, and a corresponding stabilization of the optical resonance. We show how such an effect manifests in the intensity autocorrelation $g^{(2)}(\tau)$ of scattered photons, whose long-time bunching behavior changes from quadratic decay for low photon-scattering rates (weak laser intensities) to ever slower exponential decay for increasing laser intensities as optical measurements impede the nuclear spin evolution.

DOI: 10.1103/PhysRevA.99.053853

I. INTRODUCTION

The generation of useful entanglement between photons is the central challenge in optical quantum computing schemes. Self-assembled quantum dots (QDs) have the potential to meet this challenge, either by emitting strings of entangled photons [1–3] or by mediating an effective interaction between photons via a giant phase shift [4–8]. Current experimental efforts to utilize such schemes, however, are often hindered by noise arising due to the coupling of an electron spin to the nuclear spins in the host material [9–13]. Nevertheless, the dephasing caused by these nuclear spins is qualitatively different from that caused by coupling to a photon or phonon baths, as the nuclear spins evolve slowly and unitarily on the timescale set by the electron spin dynamics, which gives rise to a variety of non-Markovian effects [13–21]. While this unique nature of the nuclear spin environment might make it possible to experimentally suppress nuclear spin noise and possibly even control them in a useful way, it also presents a formidable theoretical challenge to find reliable and insightful models of nuclear spin behavior.

We consider the effect of nuclear spins in giant phase shift experiments such as those described in Ref. [22] [see Fig. 1(a)], in which narrowband laser photons of linear polarization described by $|H\rangle \propto |L\rangle + |R\rangle$ scatter off a cavity containing a charged QD in a large ($\gtrsim$100 mT) magnetic field in the Faraday configuration. Since an electronic transition couples only to one of the two circular polarizations $|L\rangle$ and $|R\rangle$, the photon polarization state upon scattering is given by $e^{i\theta_L}|L\rangle + e^{i\theta_R}|R\rangle$, with the phase shift difference $\theta = \theta_L - \theta_R$ taking values of up to 180° [4,5,23]. Hence, a linearly polarized photon $|H\rangle$ can be reflected with the orthogonal linear polarization $|V\rangle \propto |L\rangle - |R\rangle$, as shown in Fig. 1(b). The phase shift is highly sensitive to the resonance energy of the electronic transition, which in turn depends on the nuclear spin environment via the Overhauser shift [24]. As the nuclear spin system evolves, the phase shift θ drifts over time, such that high values are observed only during short intervals ($\theta > 120°$ in 100 μs time bins [25]) but the time-averaged phase shift is low ($\langle\theta\rangle \approx 6°$ in [25]). Photon-detection events in the cross-polarized (orthogonal to input laser) channel are therefore bunched on a μs timescale, such that an intensity autocorrelation function has $g^{(2)}(\tau) < 1$ for $\tau <$ ns due to the single-photon nature of the scattered field, but $g^{(2)}(\tau) > 1$ for $\tau \sim \mu$s as the nuclear spin coupling effectively leads to blinking.

In this work, we develop a quantum optical treatment that relates the intensity correlation function in the cross-polarized channel $g^{(2)}(\tau)$ to a two-time correlation function of the nuclear spin system. We show that $g^{(2)}(\tau)$ decreases quadratically for low laser intensities, as depicted by the blue curve in Fig. 1(c). Observation of this quadratic short-time behavior would demonstrate the coherent nature of nuclear spin noise in QDs, which could help distinguish it from other possible sources of resonance fluctuations in these systems. However, the dependence of the photon phase shift on the nuclear spin state is only one aspect of a two-way interaction, as a photon-scattering event has the effect of a quantum measurement on the nuclear spin state. Incorporating this into our formalism, we find that frequent photon-scattering events, corresponding to higher driving intensities, impede the nuclear spin evolution and associated drifting of the resonance energy, which leads to a broadened intensity autocorrelation function that decays linearly with τ. This can be understood as a quantum Zeno effect [26–32], which is readily observable

*nutzat@gmail.com

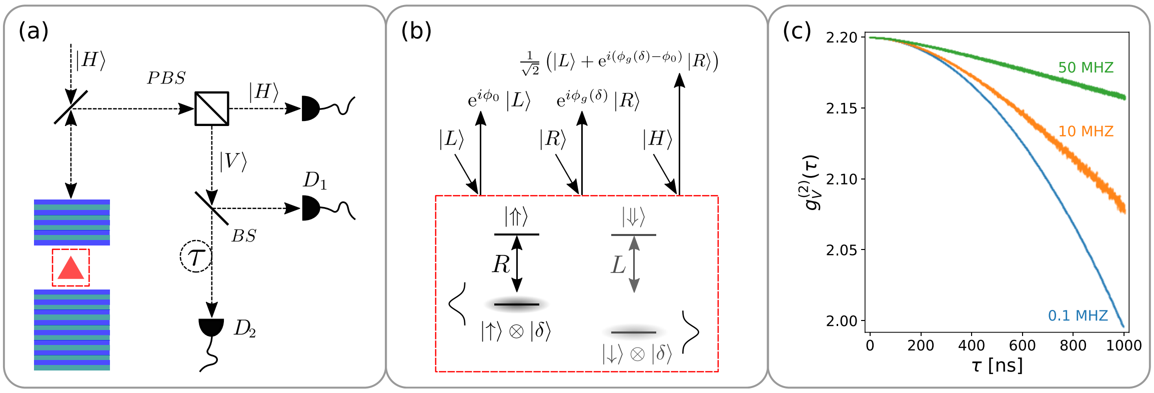

FIG. 1. (a) Experimental setup used to measure photon phase shifts due to a quantum dot inside a micropillar cavity. The states $|H\rangle$ and $|V\rangle$ denote horizontally and vertically polarized light, while (P)BS labels a (polarizing) 50:50 beam splitter. A variable delay τ between detectors D_1 and D_2 can be used to measure the intensity autocorrelation function of light scattered into a cross-polarized (vertical) channel, as shown in (c). (b) Right $|R\rangle$ and left $|L\rangle$ circularly polarized photons couple to the spin ground states $|\uparrow\rangle$ and $|\downarrow\rangle$, respectively. In a large magnetic field, the $|\downarrow\rangle$ is far detuned, and $|L\rangle$ reflects off an effectively empty cavity, while $|R\rangle$ experiences a phase shift $\phi_g(\delta)$ that depends on the nuclear spin Overhauser field δ. (c) Cross-polarized intensity correlation function for different average photon count rates obtained from a Monte Carlo simulation including eight nuclear spins. While the quadratic behavior characteristic of unitary evolution is observed for low count rates, the evolution of the nuclear spins is impeded by more frequent photon scattering, which constitutes a quantum Zeno effect. Note that the antibunching at subnanosecond timescales is neglected and that the weak-driving assumption is satisfied. Parameters A_k and ω_k were randomly drawn from a Gaussian distribution with $\langle A_k\rangle = \langle\omega_k\rangle = 0.5\ \mu$eV, $\sigma(A_k) = 0.25\ \mu$eV, and $\sigma(\omega_k) = 10$ neV.

here in an optical intensity correlation function. Experimental observation of this characteristic change in the intensity autocorrelation function would demonstrate this quantum Zeno effect and open up a measurement-based route to control nuclear spins in QDs.

II. INPUT-OUTPUT FORMALISM WITH ELECTRON-NUCLEAR SPIN COUPLING

Our aim is to calculate the cross-polarized intensity autocorrelation $g^{(2)}(\tau)$ for photons scattered off the QD-cavity system which incorporates the nuclear spin environment, and which we achieve using an extended input-output formalism [23,33,34]. We consider a continuum of optical modes described by annihilation operators $b(\omega)$ propagating towards and away from an optical cavity with frequency ω_c and associated cavity-mode operator a. The cavity mode, in turn, couples to a two-level system (TLS) with ground and excited states $|\uparrow\rangle$ and $|\Uparrow\rangle$, respectively, which itself is coupled to a bath of nuclear spins. The total Hamiltonian describing all degrees of freedom is written $H = H_0 + H_I$, with (setting $\hbar = 1$)

$$H_0 = \frac{1}{2}\omega_0\sigma^z + \omega_c a^\dagger a + \int_0^\infty d\omega\, \omega b^\dagger(\omega)b(\omega) + H_Z, \qquad (1)$$

$$H_I = g(\sigma^- a^\dagger + \sigma^+ a) + \int_0^\infty d\omega \sqrt{\kappa(\omega)}(b(\omega)a^\dagger + b^\dagger(\omega)a) + H_O, \qquad (2)$$

where $\sigma^z = |\Uparrow\rangle\langle\Uparrow| - |\uparrow\rangle\langle\uparrow|$, $\sigma^- = |\uparrow\rangle\langle\Uparrow|$, $\sigma^+ = |\Uparrow\rangle\langle\uparrow|$, ω_0 is the transition energy of the TLS, and g is the TLS-cavity coupling strength. The nuclear Zeeman term is $H_Z = \sum_j \omega_j I_j^z$, with Pauli z operator I_j^z acting on nuclear spin j and nuclear Zeeman splitting ω_j due to an external magnetic field along $\hat{z}$. The electron-nuclear coupling term is $H_O = \frac{1}{2}\sigma^z\hat{\Delta}$, with Overhauser shift operator

$$\hat{\Delta} = \sum_j A_j I_j^z + \frac{1}{2\omega}\sum_{m\neq n} A_m A_n I_m^+ I_n^-, \qquad (3)$$

which results from a Schrieffer-Wolff transformation on the contact hyperfine Hamiltonian given in Eq. (41) [35]. Note that while the contact hyperfine interaction involves two electron spin states, $|\uparrow\rangle$ and $|\downarrow\rangle$, here we focus on one of these ground states only, arbitrarily labeled $|\uparrow\rangle$. Neglecting the other spin state $|\downarrow\rangle$ is justified in a large ($\gtrsim$100 mT) magnetic field, where energy conservation prevents flip flops between these electron spin states which are separated by the electron Zeeman energy ω.

We approximate the cavity-port-mode coupling strength as a constant $\sqrt{\kappa(\omega)} \approx \sqrt{\kappa(\omega_c)} \equiv \sqrt{\kappa}$ over the relevant optical frequencies, and in doing so we find the Heisenberg equations of motion,

$$\dot{\sigma}^-(t) = ig\, a(t)\sigma_z(t) - i[\omega_0 + \hat{\Delta}(t)]\sigma^-(t), \qquad (4a)$$

$$i\,\dot{a}(t) = (\omega_c - i\pi\kappa)a(t) + g\sigma^-(t) + \sqrt{\kappa}\, b_{\rm in}(t), \qquad (4b)$$

$$2\pi i\sqrt{\kappa}\, a(t) = b_{\rm in}(t) - b_{\rm out}(t), \qquad (4c)$$

where we have defined the incoming and outgoing field operators as $b_{\rm in}(t) = \int d\omega\, b_0(\omega)\exp(-i\omega t)$ with $b_0(\omega) \equiv b(\omega, t_0)$, and $b_{\rm out}(t) = \int d\omega\ b_1(\omega)\exp(-i\omega t)$ with $b_1(\omega) \equiv b(\omega, t_1)$ [34], and extended frequency integrals such that $\int_0^\infty d\omega \to \int_{-\infty}^\infty d\omega \equiv \int d\omega$. Taking the Fourier transform of Eq. (4b), we find

$$(\omega - \omega_c + i\pi\kappa)a(\omega) = g\sigma^-(\omega) + \sqrt{\kappa}b_0(\omega), \qquad (5)$$

where $\sigma^-(t) = \int d\omega\, \sigma^-(\omega)e^{-i\omega t}$, and similarly for $a(t)$.

The standard procedure in input-output theory is to use the Fourier transform of Eq. (4a) to replace $\sigma^-(\omega)$ in Eq. (5), which is then used in the Fourier transform of Eq. (4c),

$b_{\rm in}(\omega) - b_{\rm out}(\omega) = 2\pi i\sqrt{\kappa}a(\omega)$, to find a relationship between frequency components of the incoming and outgoing fields $b_{\rm in}(\omega)$ and $b_{\rm out}(\omega)$. We use a similar procedure here, but note that the occurrence of the time-dependent Overhauser shift operator $\hat{\Delta}(t)$ in Eq. (4a) means there is no simple relationship between the Fourier components $\sigma(\omega)$ and $a(\omega)$. Instead, we arrive at the integral equation

$$\int d\omega\{[\omega - \hat{\omega}_0(t)]\sigma^-(\omega) - ga(\omega)\}e^{-i\omega t} = 0, \tag{6}$$

where we have defined $\hat{\omega}_0(t) \equiv \omega_0 + \hat{\Delta}(t)$ and made the approximation $\sigma_z \approx -1$, valid for weak driving. Combining Eqs. (5) and (6) then gives

$$\int d\omega e^{-i\omega t}\hat{f}_+(\omega, t)a(\omega) = \int d\omega e^{-i\omega t}\sqrt{\kappa}[\omega - \hat{\omega}_0(t)]b_0(\omega), \tag{7}$$

where $\hat{f}_\pm = (\omega - \omega_c \pm i\pi\kappa)[\omega - \hat{\omega}_0(t)] - g^2$. Using this in the Fourier transformation of Eq. (4c) leads to

$$\int d\omega\{b_{\rm out}(\omega)\hat{f}_+(\omega, t) - b_{\rm in}(\omega)\hat{f}_-(\omega, t)\}e^{-i\omega t} = 0. \tag{8}$$

When the Overhauser term is neglected, $\hat{\Delta}(t) = 0$, Eq. (8) simplifies to $b_{\rm out}(\omega) = r(\omega)b_{\rm in}(\omega)$ with the scalar $r(\omega) = f_-(\omega)/f_+(\omega)$, which is the well-known cavity-QED reflection coefficient [23]. An analogous result relating incoming and outgoing fields in the presence of nuclear spin coupling can be obtained by assuming a slowly varying Overhauser shift. To see this, we consider attempting to isolate the integrand in Eq. (8) by performing the finite-domain definite integral,

$$\int_{t_c-t_\Delta}^{t_c+t_\Delta} dt e^{i\omega' t}\int d\omega\, b_{\rm out}(\omega)\hat{f}_+(\omega, t)e^{-i\omega t} = \int_{t_c-t_\Delta}^{t_c+t_\Delta} dt e^{i\omega' t}\int d\omega\, b_{\rm in}(\omega)\hat{f}_-(\omega, t)e^{-i\omega t}. \tag{9}$$

Choosing the integration range such that $t_\Delta \ll t_{\rm fluc}$, where $t_{\rm fluc}$ is the characteristic timescale of the Overhauser field fluctuations, we can approximate $\hat{\Delta}(t) \approx \hat{\Delta}(t_c)$ in the integrands and arrive at

$$\int d\omega\, b_{\rm out}(\omega, t_c)\hat{f}_+(\omega, t_c)t_\Delta {\rm sinc}[t_\Delta(\omega - \omega')] = \int d\omega\, b_{\rm in}(\omega, t_c)\hat{f}_-(\omega, t_c)t_\Delta {\rm sinc}[t_\Delta(\omega - \omega')], \tag{10}$$

where $b_{\rm out}(\omega, t_c) \equiv b_{\rm out}(\omega)e^{-i\omega t_c}$, and similarly for $b_{\rm in}(\omega, t_c)$. If the Overhauser shift fluctuates slowly, then we can choose the spectral width of the sinc function in Eq. (10), t_Δ^{-1}, to be much narrower than the width of the function $\hat{f}_\pm(\omega, t_c)$. We then find

$$\tilde{b}_{\rm out}(\omega) = \hat{r}(\omega, t) \otimes \tilde{b}_{\rm in}(\omega), \tag{11}$$

with $\hat{r}(\omega, t) = f_+(\omega, t)^{-1}f_-(\omega, t)$ and given by

$$\hat{r}(\omega, t) = \mathbb{1} + \frac{2i\pi\kappa[\omega_0 + \hat{\Delta}(t) - \omega]}{(\omega_c - \omega - i\pi\kappa)[\omega_0 + \hat{\Delta}(t) - \omega] - g^2}, \tag{12}$$

while the incoming and outgoing field operators are now defined as

$$\tilde{b}_{\rm out}(\omega) \equiv \int d\omega'\, b_{\rm out}(\omega', t)t_\Delta {\rm sinc}[(\omega - \omega')t_\Delta], \tag{13}$$

and similarly for $\tilde{b}_{\rm in}(\omega)$. Noticing the convolution form of this expression, we see that this operator can be thought of as a broadened version of its exact frequency counterpart $b_{\rm out}(\omega)$ owing to the finite integration time t_Δ.

The relationship between incoming and outgoing fields given in Eq. (11) is our first result, and generalizes the input-output theory to systems with slowly varying resonance energies. It is valid if the integration time t_Δ in Eq. (9) satisfies $t_{\rm fluc} \gg t_\Delta \gg 1/w_f$, where $t_{\rm fluc}$ is the fluctuation time of the Overhauser shift and w_f is the spectral width of the phase shift feature, which is obtained by considering the frequency dependence of $\hat{f}_\pm(\omega, t) = \hat{f}(\omega, t)\exp[\pm i\hat{\theta}(\omega, t)]$. We find that the phase factor varies most rapidly at $\omega = \omega_c = \hat{\omega}_0$, at which point

$$\frac{d}{d\omega}\hat{\theta}(\omega, t) = 2\pi\frac{\kappa}{g^2}, \tag{14}$$

and $\frac{d}{d\omega}\hat{f}(\omega, t) = 0$. As such, the fractional variation $\frac{d}{d\omega}\hat{f}(\omega, t)/\hat{f}(\omega, t)$ does not exceed a bound of the order of κ/g^2 when considering laser-QD detunings no greater than $\omega - \hat{\omega}_0(t) \approx g^2/\kappa$, and laser-cavity detunings limited to $\omega - \omega_c \approx \kappa$. The functions $\hat{f}_\pm(\omega, t)$ therefore vary on a frequency scale given by the linewidth g^2/κ of the TLS transition. This linewidth is typically of the order of a few GHz for QD experiments, while the Overhauser shift fluctuation time can be estimated to be hundreds of milliseconds based on [25], such that $t_{\rm fluc} \gg t_\Delta \gg 1/w_f$ can be satisfied and Eq. (11) is applicable to QD experiments. We interpret t_Δ as a parameter that adjusts the tradeoff between frequency and time resolution of our theory. Equation (11) relates Fourier components $\tilde{b}_{\rm in/out}(\omega)$ that must be understood as averages of the exact Fourier components of the incoming and outgoing fields over a bandwidth interval $1/t_\Delta \gg 1/t_{\rm fluc}$. For an experiment with a QD linewidth of 1 GHz and a fluctuation time of 1 μs, our theory describes effects with a resolution of up to ~1 MHz in frequency and ~1 ns in time.

III. OPTICALLY MEASURED NUCLEAR TWO-TIME CORRELATION FUNCTION

Having established how frequency components in the incoming and outgoing fields are affected by the nuclear spin bath, we now use this result to show how a measured optical intensity autocorrelation depends on a correlation function of the nuclear spins. We consider the optical intensity autocorrelation function of the cross-polarized reflected light. Assuming a horizontally polarized input field, the correlation in the vertical polarized orientation is proportional to the second-order correlation function,

$$G_V^{(2)}(t, t+\tau) = {\rm Tr}_{\rm tot}[E_V^{(-)}(t)E_V^{(-)}(t+\tau)E_V^{(+)}(t+\tau)E_V^{(+)}(t)\chi], \tag{15}$$

where $E_V^{(\pm)}(t)$ are the positive- and negative-frequency components of the vertically polarized electric field at time t, and the trace is performed over the total port-mode–cavity–electron spin–nuclear spin system, with total initial state χ, and where the Heisenberg electric-field operators evolve unitarily in this complete Hilbert space.

To proceed, we express these field operators as

$$E_V^{(+)}(t) = \int_0^\infty d\omega\, \tilde{b}_{\mathrm{out}}^V(\omega, t), \tag{16}$$

where we have neglected numerical factors and retardation effects. Following Eq. (11), a cavity containing a QD with electron spin projection $|\uparrow\rangle$ reflects a right circularly polarized photon according to $\tilde{b}_{\mathrm{out}}^R(\omega, t) = \hat{r}(\omega, t) \otimes \tilde{b}_{\mathrm{in}}^R$, while a left circularly polarized photon acquires a phase shift $r_0(\omega) = \hat{r}(\omega, t)|_{g=0}$ corresponding to an empty cavity. Hence we can write

$$\tilde{b}_{\mathrm{out}}^V(\omega, t) = \hat{r}_{\mathrm{cr}}(\omega, t) \otimes \tilde{b}_{\mathrm{in}}^H(\omega) + \hat{r}_{\mathrm{co}}(\omega, t) \otimes \tilde{b}_{\mathrm{in}}^V(\omega), \tag{17}$$

where the operators $\hat{r}_{\mathrm{co/cr}}(\omega, t) = \frac{1}{2}[\hat{r}(\omega, t) \pm r_0(\omega)]$ give the reflectivities into the co- and cross-polarized channels, which depend on the nuclear spin state through the dependence of $\hat{r}(\omega, t)$ on the Overhauser operator $\hat{\Delta}(t)$. We assume an initial state $\chi = |H(\omega)\rangle\, \langle H(\omega)| \otimes \rho_a \otimes |\uparrow\rangle\, \langle\uparrow| \otimes \rho_N$, where $|H(\omega)\rangle$ satisfying $\tilde{b}_{\mathrm{in}}^H(\omega')\, |H(\omega)\rangle = \beta\delta(\omega - \omega')\, |H(\omega)\rangle$ is a horizontally polarized coherent state of amplitude β; ρ_a and ρ_N are states of the cavity-mode and nuclear spin system, respectively, and the electron is assumed to remain in state $|\uparrow\rangle$ during the measurement. Substituting this state into Eq. (15) gives

$$\begin{aligned} G_V^{(2)}(t, t+\tau) = {} & |\beta|^4 \mathrm{Tr}[\hat{r}_{\mathrm{cr}}^\dagger(\omega, t)\hat{r}_{\mathrm{cr}}^\dagger \\ & \times (\omega, t+\tau)\hat{r}_{\mathrm{cr}}(\omega, t+\tau)\hat{r}_{\mathrm{cr}}(\omega, t)\rho_N], \end{aligned} \tag{18}$$

where now and in all that follows the trace is taken only over the nuclear degrees of freedom, showing that we have related an optically measured quantity to a nuclear two-time correlation function. This correlation function gives the joint probability to measure two photons scattered into the cross-polarization channel at times t and at $t+\tau$. It is a *nonexclusive probability*, as it does not suppose anything regarding any intermediate scattering events, into the cross-polarization channel or otherwise [36]. Its nonexclusive nature is evidenced by the globally unitary evolution of the full Heisenberg picture operator $E_V^{(-)}(t)$, which depends on the systems involved, including the photonic degrees of freedom. A nonexclusive correlation function is the correct form to make a connection with experiments, as typically one does not have access to a full scattering history, and in practice we take a statistical average over any intermediate scattering events.

However, we are interested here in how individual scattering events affect the nuclear spin environment, which in turn affects later scattering events. We therefore seek a relationship between the measured nonexclusive correlation function in Eq. (18) and an *exclusive* correlation function, which gives a conditional probability corresponding to a fixed number of scattering events at fixed times [36]. Such a relationship can be expressed as

$$\begin{aligned} G_V^{(2)}(t, t+\tau) = {} & \sum_{n=0}^{\infty} \sum_{\{c_i\}} \int_t^{t+\tau} dt_n \int_t^{t_n} dt_{n\text{-}1} \ldots \\ & \times \int_t^{t_2} dt_1\, \mathcal{G}_{V,\{c_i\},V}^{(n)}(t, t_1, \ldots, t_n, t+\tau), \end{aligned} \tag{19}$$

where $\mathcal{G}_{V,\{c_i\},V}^{(n)}(t, t_1, \ldots, t_n, t+\tau)$ is the exclusive probability density that exactly $n+2$ photon-scattering events take place in the interval $[t, t+\tau]$, with the first and last photons scattered into vertical polarization at times t and $t+\tau$, and n additional photons scattered at intermediate times $t_1, \ldots, t_n$ into polarizations labeled $\{c_i\} = c_1, \ldots, c_n$, with c_i being either the co- (H) or cross-polarized (V) channel. We now decompose the exclusive probability $\mathcal{G}$ into probabilities describing the scattering times and the scattering polarizations. We write

$$\begin{aligned} & \mathcal{G}_{V,\{c_i\},V}^{(n)}(t, t_1, \ldots, t_n, t+\tau) \\ & \quad = p_t(t, t+\tau; n)\, p_t(t_1, \ldots, t_n)\, p_c(V, \{c_i\}, V), \end{aligned} \tag{20}$$

where $p_t(t, t+\tau; n)$ is the nonexclusive probability of photon-scattering events at t and $t+\tau$, with n intermediate scattering events at unspecified times, $p_t(t_1, \ldots, t_n)$ the probability density of these intermediate events occurring at $t_1, \ldots, t_n$, and $p_c(V, \{c_i\}, V)$ the probability of these photons scattered into polarizations $V, c_1, \ldots, c_n, V$. For a coherent input state $|H(\omega)\rangle$ such as we consider, the probability of exactly n scattering events occurring in the interval $[t, t+\tau]$ is given by a Poisson distribution $p(n, \tau)$, which depends on the coherent-state amplitude β (related to laser power) and the duration τ, while the scattering times are random and uncorrelated. This allows us to write $p_t(t, t+\tau; n) = G^{(1)}(t)G^{(1)}(t+\tau)p(n, \tau)$ and $p_t(t_1, \ldots, t_n) = n!/\tau^n$, where $G^{(1)}(t)$ is the photon-scattering rate. The normalized (nonexclusive) cross-polarized intensity correlation function can therefore be written as

$$\begin{aligned} g^{(2)}(\tau) &= \frac{G_V^{(2)}(t, t+\tau)}{G_V^{(1)}(t)G_V^{(1)}(t+\tau)} \\ &= \sum_{n=0}^{\infty} p(n, \tau)\frac{n!}{\tau^n} \int_t^{t+\tau} dt_n \int_t^{t_n} dt_{n\text{-}1} \cdots \int_t^{t_2} dt_1 \\ & \quad \times \sum_{\{c_i\}} \frac{p_c(V, \{c_i\}, V)}{p_V(t)p_V(t+\tau)}, \end{aligned} \tag{21}$$

where $G_V^{(1)}(t) = p_V(t)G^{(1)}(t)$, with $p_V(t)$ the probability that a photon scattered at time t is detected in the vertically polarized channel. Written in this way, we see that the normalized cross-polarized two-time correlation function is the joint probability for two photons to scatter into the cross polarization at times t and $t+\tau$, averaged over all possible numbers, timings, and polarization channels of intermediate events.

The joint probability $p_c(V, \{c_i\}, V)$ appearing in Eq. (21) is an exclusive quantity describing the likelihood that exactly $n+2$ photons scatter at times $t, t_1, \ldots, t_n, t+\tau$ with polarizations $V, c_1, \ldots, c_n, V$, and can be shown to depend on the nuclear spin system alone. To see this, we must understand how the detection of a photon affects the state of the nuclear system, and combine this effect with the appropriate nuclear spin evolution between scattering events. In the former case, let us consider the implication of the scattering process described in Eq. (17). We consider an initially horizontally polarized photon and a nuclear spin state $|\delta\rangle$, giving an initial state $\tilde{b}_{\mathrm{in}}^H(\omega)^\dagger\, |0\rangle \otimes |\delta\rangle$, with $|0\rangle$ the vacuum. If $|\delta\rangle$ is

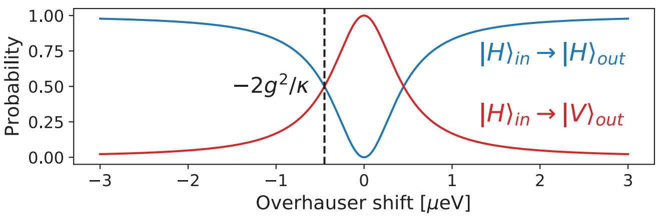

FIG. 2. Probability for a photon-scattering event into the copolarized $H \rightarrow H$ (blue) or cross-polarized $H \rightarrow V$ channel $\langle\delta|M_c^\dagger M_c|\delta\rangle$, shown for a nuclear system in an Overhauser shift eigenstate $|\delta\rangle$, and as a function of the shift δ. For zero Overhauser shift, cross-polarized photons are preferred, with this bias reversing as the Overhauser shift becomes greater than the linewidth of the electronic transition in the cavity $2g^2/\kappa$. Parameters (μeV): $\kappa = 4000$, $g = 30$, $\omega_c = \omega_0 = \omega$.

an eigenstate of the Overhauser shift operator $\hat{\Delta}$, we can write $\hat{r}_c(\omega)\,|\delta\rangle = r_c^\delta\,|\delta\rangle$, with the subscript indicating the co- or cross-polarized channel. The state after scattering is then given by

$$\tilde{b}_{\text{out}}^H(\omega)^\dagger\,|0\rangle \otimes |\delta\rangle = \left[r_{\text{cr}}^\delta \tilde{b}_{\text{in}}^V(\omega)^\dagger + r_{\text{co}}^\delta \tilde{b}_{\text{in}}^H(\omega)^\dagger\right]|0\rangle \otimes |\delta\rangle\,. \tag{22}$$

From this, we see that destructive (absorptive) detection of a co- or cross-polarized photon from a general nuclear state $|\psi\rangle$ then results in an (unnormalized) postmeasurement state $|\psi'\rangle = M_c\,|\psi\rangle$, with operators

$$M_c = \sum_\delta r_c^\delta\,|\delta\rangle\,\langle\delta|\,. \tag{23}$$

These operators can be interpreted as measurement operators describing the effect of a photon-scattering event on the nuclear spin system. The weights of the associated positive-operator valued measurement (POVM) elements are shown in Fig. 2.

Between scattering events, since the probability $p(V, \{c_i\}, V)$ is conditioned on photon-scattering events happening only at times $t_1, \ldots, t_n$, the nuclear spin evolution is the unitary evolution generated by the Hamiltonian $H_N = H_Z + \hat{\Delta}/2$, where the Zeeman Hamiltonian H_Z and Overhauser shift operator $\hat{\Delta}$ are defined in Eqs. (2) and (3). This allows us to write

$$p(V,\{c_i\}, V) = \text{Tr}\left[\Phi_V \mathcal{U}_{n+1}\left(\prod_{i=1}^n \Phi_{c_i}\mathcal{U}_i\right)\Phi_V\,\rho_N(t)\right], \tag{24}$$

where the superoperators Φ_{c_i} and $\mathcal{U}_i$ act as

$$\begin{aligned}\Phi_c\rho &= M_c\;\rho\;M_c^\dagger,\\ \mathcal{U}_i\rho &= e^{-iH_N\Delta_i}\rho\,e^{iH_N\Delta_i},\end{aligned} \tag{25}$$

and we define $\Delta_i \equiv t_i - t_{i\text{-}1}$, $t_0 \equiv t$, and $t_{n+1} \equiv t + \tau$. The probability in Eq. (24) is exclusive and corresponds to one possible scattering history. The average over all such histories gives the measured two-time correlation function following Eq. (21). We note that it is the statistical mixture of these histories, and not their coherent superposition, that determines the observed behavior, as for the nuclear spin system the photon-scattering events are irreversible measurement processes. This formulation is analogous to the quantum jump approach [36,37].

IV. ZENO EVOLUTION OF THE NUCLEAR TWO-TIME CORRELATION FUNCTION

We are now in a position to explore the behavior of the normalized correlation function $g^{(2)}(\tau)$ given in Eq. (21). We begin by examining the regime of low laser power. In this regime, we can assume that the probability of intermediate scattering events in a time interval τ vanishes, i.e., $p(0, \tau) \approx 1$ and $p(n \geqslant 1, \tau) \approx 0$, while the factor involving the product in Eq. (24) is the identity. Equation (21) then gives

$$g^{(2)}(\tau) \approx \frac{p_c(V, \{\}, V)}{p_V(t)p_V(t+\tau)} = \frac{\text{Tr}(O_V\mathcal{U}_{0\to\tau}\varrho)}{\text{Tr}(O_V\,\rho_N)^2}, \tag{26}$$

where we assume the nuclear system is in a steady state, i.e., $\rho(t) = \rho(t+\tau) = \rho_N$, the POVM element is $O_V = M_V^\dagger M_V$, and we have defined the unnormalized state $\varrho = \Phi_V\rho_N$. The steady-state assumption allows us to take $t = 0$ without loss of generality. Expanding the unitary propagator $\mathcal{U}_{0\to\tau}$ to second order, we find

$$\text{Tr}(O_V\mathcal{U}_{0\to\tau}\varrho) \approx \text{Tr}\big(O_V^2\rho_N\big) - \frac{1}{2\tau_z^2}\tau^2, \tag{27}$$

where the linear term in τ vanishes under the assumption that the steady state has no coherence in the Overhauser shift eigenbasis, i.e., $[O_V, \rho_N] = 0$, and we have defined the nuclear Zeno time,

$$\tau_z = 1/\sqrt{\text{Tr}(O_V[H_N, [H_N, \varrho]])}. \tag{28}$$

The quadratic short-time behavior seen in Eq. (27) is characteristic of any unitary evolution, and its experimental observation would be a signature of the non-Markovian nature of the nuclear spin bath and help to distinguish it from other sources of resonance fluctuations. Furthermore, identification of the timescale of the nuclear spin evolution, given by the Zeno time τ_z, would provide valuable information on the dynamical behaviour of the nuclear spin system itself.

For laser powers beyond the low-intensity regime, we need to take intermediate scattering events into account. Averaging over the polarization orientation of the n intermediate events gives the polarization-averaged exclusive probability, which we write as

$$\mathcal{P}_n = \sum_{\{c_i\}} p(V, \{c_i\}, V) = \text{Tr}(O_V V_\tau\varrho), \tag{29}$$

with superoperator $V_\tau \equiv \mathcal{U}_{n+1}\prod_{i=1}^n \Phi\,\mathcal{U}_i$. Here the superoperator Φ describes a photon-scattering event as a nonselective measurement, and acts as

$$\Phi\;\rho = M_V\rho M_V^\dagger + M_H\rho M_H^\dagger. \tag{30}$$

Such a nonselective measurement takes a nuclear state ρ and rescales all coherences in the Overhauser shift eigenstate basis $\langle\delta|\rho|\delta'\rangle$ by a factor,

$$r_{\delta\delta'} = r_{\text{co}}^\delta\big(r_{\text{co}}^{\delta'}\big)^* + r_{\text{cr}}^\delta\big(r_{\text{cr}}^{\delta'}\big)^* \equiv |r_{\delta\delta'}|\exp(i\theta_{\delta\delta'}). \tag{31}$$

This factor can be interpreted as an indistinguishability measure relating the states $|\delta\rangle$ and $|\delta'\rangle$. If both states scatter a photon into the same polarization, then they cannot be distinguished by photon scattering and $r_{\delta\delta'} = 1$. On the other hand, if the photons scattered off $|\delta\rangle$ are orthogonal to photons scattered off $|\delta'\rangle$, then photon scattering has the effect of a projective measurement with discarded outcome. In the first case, the coherence between $|\delta\rangle$ and $|\delta'\rangle$ remains untouched, while in the latter case, the coherence is completely destroyed.

We calculate the probability $\mathcal{P}_n$ to second order in the time intervals Δ_i. To do so, we first expand the first time evolution and measurement step to arrive at

$$V_\tau \varrho = \mathcal{U}_{n+1} \prod_{i=2}^{n} \Phi\, \mathcal{U}_i \big(\varrho + \varrho_1^{(1)} + \varrho_1^{(2)}\big), \tag{32}$$

where the subscripts indicate the state after the first intermediate photon-scattering event, and we have defined the first- and second-order contributions as $\varrho_1^{(1)} = -i\Delta_1 \Phi([H_N, \varrho])$ and $\varrho_1^{(2)} = -(\Delta_1^2/2)\Phi([H_N, [H_N, \varrho]])$. Expanding the subsequent steps $\Phi\, \mathcal{U}_i$ and discarding terms of cubic order yields the recursion relations

$$\varrho_k^{(1)} = \Phi \varrho_{k\text{-}1}^{(1)} - i\Delta_k \Phi([H_N, \varrho]), \tag{33a}$$

$$\varrho_k^{(2)} = \Phi \varrho_{k\text{-}1}^{(2)} - i\Delta_k \Phi\big(\big[H_N, \varrho_{k\text{-}1}^{(1)}\big]\big) - \frac{\Delta_k^2}{2}\Phi([H_N, [H_N, \varrho]]). \tag{33b}$$

In terms of these density operator contributions, Eq. (29) becomes

$$\begin{aligned}\mathcal{P}_n &= \mathrm{Tr}\big[O_V \mathcal{U}_{n+1}\big(\varrho + \varrho_n^{(1)} + \varrho_n^{(2)}\big)\big]\\ &= \mathrm{Tr}[O_V \varrho] + \mathrm{Tr}\big[O_V \varrho_{n+1}^{(2)}\big],\end{aligned} \tag{34}$$

where we make use of the identities $\mathrm{Tr}[\Phi A] = \mathrm{Tr}[A]$, $\mathrm{Tr}[\Phi(O_V A)] = \mathrm{Tr}[O_V \Phi(A)]$ for any operator A, and $\mathrm{Tr}[O_V \rho_k^{(1)}] = 0$. The recursion relations have the solutions

$$\varrho_k^{(1)} = -i \sum_{j=1}^{k} \Delta_j \Phi^{k\text{-}j+1}([H_N, \varrho]), \tag{35a}$$

$$\begin{aligned}\varrho_k^{(2)} = &-\sum_{j=1}^{k} \frac{\Delta_j^2}{2} \Phi^{k\text{-}j+1}([H_N, [H_N, \varrho]])\\ &-i \sum_{j=1}^{k} \Delta_j \Phi^{k\text{-}j+1}\big(\big[H_N, \varrho_{j\text{-}1}^{(1)}\big]\big),\end{aligned} \tag{35b}$$

which lead to

$$\mathcal{P}_n = \mathrm{Tr}\big(O_V V_{t_n} \varrho\big) - (\tau - t_n) S_n - \frac{(\tau - t_n)^2}{2\tau_Z^2}, \tag{36}$$

where we define the slope function

$$S_n \equiv \sum_{j=1}^{n} \Delta_j \mathrm{Tr}(O_V [H_N, \Phi^{n\text{-}j+1}[H_N, \varrho]]), \tag{37}$$

and where

$$\mathrm{Tr}(O_V V_{t_n} \varrho) = \mathrm{Tr}\big(O_V^2 \rho_N\big) - \sum_{k=1}^{n} \Delta_k S_{k\text{-}1} - \sum_{k=1}^{n} \frac{\Delta_k^2}{2\tau_Z^2}. \tag{38}$$

Equation (36) constitutes the major result of this work. It gives the joint probability of two photons being detected in the vertical (crossed) polarization channel at times 0 and τ, given n scattering events of unknown polarization scattering at intermediate times $\{t_i\}$. Following Eq. (21), averaging over the number and timing of these intermediate events gives the experimentally measurable cross-polarized intensity autocorrelation function $g_V^{(2)}(\tau)$ shown in Fig. 1(c).

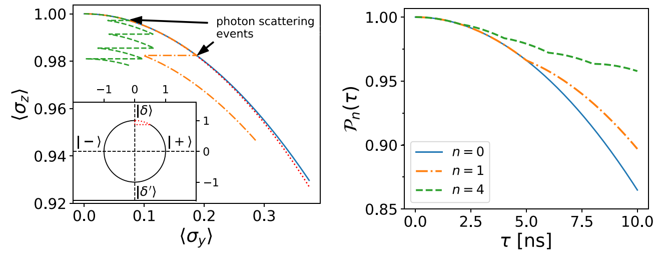

FIG. 3. Left: Representative time evolution of the nuclear spin system, here taken to be two spins spanned by the phase shift eigenstates $|\delta\rangle$ and $|\delta'\rangle$, with the dynamics generated following Eqs. (35a) and (35b). The plot shows the path of a Bloch vector representation of the nuclear spin state, with Overhauser amplitude and coherence operators respectively $\sigma_z = |\delta\rangle\langle\delta| - |\delta'\rangle\langle\delta'|$, $\sigma_y = |+\rangle\langle+| - |-\rangle\langle-|$, with $|\pm\rangle = |\delta\rangle \pm i|\delta'\rangle$. State trajectories are shown for no photon-scattering events (blue), photon scattering every $\Delta = 5$ ns (orange) and $\Delta = 2$ ns (green). The dotted red line shows the surface of the Bloch sphere, a cross section of which is shown in the inset (red section near the pole corresponds to the outer plot). Right: Exclusive joint probability $\mathcal{P}_n$ following Eq. (36) of scattering into cross polarization at times 0 and τ corresponding to the state evolution shown to the left, where $\mathcal{P}_n \propto \langle\sigma_z\rangle$. Parameters: $A_1 = 1$, $A_2 = 3$, $\omega_1 = 2.5$, $\omega_1 = 0.5$, $\omega = 40$.

The linear and quadratic terms in Eq. (36) can be understood in terms of a generalized quantum Zeno effect. As can be seen by the vanishing trace of $\varrho_k^{(1)}$ given in Eq. (35a), the linear order time evolution only affects the coherences of the unnormalized state ϱ. Each measurement Φ reduces a coherence $\langle\delta'|\varrho_k^{(1)}|\delta\rangle$ by a factor of $r_{\delta\delta'}$, such that a particular coherence follows a sawtooth pattern shown in Fig. 3. The gradient of $\mathcal{P}_n$ at time τ depends on a commutator of the form $[H_N, \varrho_{\mathrm{coh}}]$, where $\varrho_{\mathrm{coh}} \sim \Phi^{n-j+1}[H_N, \varrho]$ is all the coherence that has accumulated up to τ. This coherence has one contribution from the evolution since the last measurement at t_n, which leads to the quadratic term in Eq. (36), and another contribution due to all the coherence that has partially "survived" the previous measurements, and is given by the linear term. The exponent of Φ gives the number of measurements that the coherence accumulated during interval Δ_j has suffered after the nth measurement.

In the limiting case of the polarization of scattered photons being independent of the nuclear spin state, the nuclear spin coherence is not affected by scattering. It is readily seen that for $\Phi([H_N, \rho_N^V]) = [H_N, \rho_N^V]$, the slope function becomes $S_n = t_n/\tau_Z^2$ and the quadratic time evolution of Eq. (27) is recovered. In general, however, an intermediate scattering event and associated measurement reduces the coherence, which decreases S_n, and therefore leads to a reduced slope of $\mathcal{P}_n$. This process can be interpreted as the system partially losing its "memory" of the previous time evolution stored as coherence.

In the opposite limit, in which projective measurements are made at evenly spaced time intervals $\Delta = \tau/n$, coherences are completely destroyed, leading to $S_n = 0$, and we find

$$\mathcal{P}_n \approx \mathrm{Tr}\big(O_v^2 \rho_N\big) - \frac{\Delta}{2\tau_Z^2}\tau. \tag{39}$$

This linear short-time evolution is characteristic of the Markovian regime, in which the system "forgets" all previous time evolutions with every scattering event. The slope of this linear time evolution decreases with the number n of measurements, such that frequent photon scattering can stabilize the nuclear system in a state that maintains resonance. This nuclear spin behavior constitutes a quantum Zeno effect. It is different from previously considered quantum Zeno effects, as the measurements implemented by single photon scattering events take place at random times and have a limited precision, thus allowing for a relatively simple experiment. The results of a Monte Carlo simulation of $g^{(2)}(\tau)$ which averages over the intermediate scattering histories are shown in Fig. 1(c) and demonstrate the characteristic flattening of the correlation function with increasing laser power, which is the experimental signature of this nuclear quantum Zeno effect.

V. NUCLEAR QUANTUM ZENO DYNAMICS IN THE PRESENCE OF MARKOVIAN NOISE

The nuclear quantum Zeno dynamics described above arise from unitary evolution of the nuclear spin system and the resulting non-Markovian behavior of the fluctuating excitonic resonance energy. However, in typical QD experiments, other sources of noise may be present which lead to dephasing of the exciton, and which are Markovian and memoryless on the timescale of the nuclear spin evolution. In particular, fluctuating charges in the vicinity of the QD can dephase the excitonic state [10], and also phonons can perturb the excitonic transition [38]. To investigate the effects of Markovian dephasing noise, we add a random, time-varying shift $s(t)$ to the resonance energy ω_0 that takes on a particular value with probability $p(s)$. This shift leads to dephasing of the excitonic state, as the phase of that state evolves in proportion to the exciton energy. Given the random shift of this energy, the phase undergoes a random walk and the average state dephases at a rate $\gamma = t_c\sigma^2/2$, where σ^2 is the variance of the shift probability distribution $p(s)$ and t_c is the characteristic timescale of the fluctuations. In our case, it is the typical magnitude σ of the shift rather than the dephasing rate γ which affects the nuclear spin evolution, as explained below.

Given a nuclear spin state $|\delta\rangle$ and a random energy shift s, a horizontally polarized photon $|H\rangle$ is scattered into a polarization state $r_{\mathrm{cr}}^{\delta+s}|V\rangle + r_{\mathrm{co}}^{\delta+s}|H\rangle$ with probability $p(s)$, where $r_{\mathrm{co/cr}}^{\delta+s}$ are the reflection coefficients into co- or cross polarization, respectively [cf. Eq. (22)]. The probability p_{cr} of photon scattering into cross polarization is then associated with a modified POVM element, $\tilde{O}_V = \sum_\delta \sum_s p(s)|r_{\mathrm{cr}}^{\delta+s}|^2\,|\delta\rangle\langle\delta|$, and the nuclear spin state upon scattering is obtained by the quantum operation $\tilde{\Phi}_V$ with operators $\{M_V^s = \sqrt{p(s)}\sum_\delta r_{cr}^{\delta+s}\,|\delta\rangle\langle\delta|\}$, i.e.,

$$\rho_{\mathrm{cr}}' = \frac{1}{p_{\mathrm{cr}}}\tilde{\Phi}_V\rho = \frac{1}{\mathrm{Tr}(\tilde{O}_V\rho)}\sum_s M_V^s\rho\big(M_V^s\big)^\dagger \tag{40}$$

[cf. Eqs. (23) and (26)]. The random resonance shift s effectively broadens the resonant feature in the polarization rotation. Replacing the POVM element O_V and quantum operation Φ in Eq. (29) by their stochastic versions $\tilde{O}_V$ and $\tilde{\Phi}$ then yields a modified cross-polarized intensity autocorrelation $g_V^{(2)}(\tau)$.

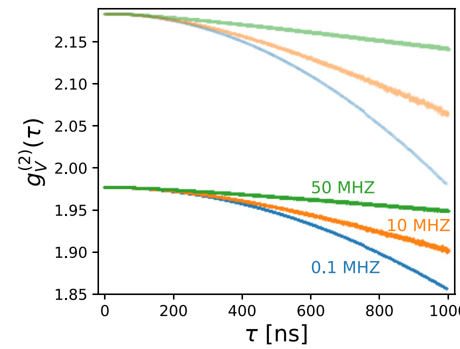

FIG. 4. Cross-polarized optical intensity autocorrelation $g_V^{(2)}(\tau)$ including Markovian resonance fluctuations noise. The transparent lines show the data from Fig. 1(c) without Markovian noise for comparison. A random, uncorrelated resonance shift s is sampled from a Gaussian distribution with zero mean and 250 MHz variance at each photon-scattering event of the Monte Carlo simulation, with all other parameters as in Fig. 1(c).

The result of a Monte Carlo simulation including these Markovian processes is shown in Fig. 4, and we see that they have a twofold effect on the intensity autocorrelation. First, the bunching seen at $\tau = 0$ is reduced, which is a consequence of the Markovianity of the noise on the timescale of the nuclear spin evolution. A cross-polarized photon detection projects the nuclear spin system into a state with significantly increased probability weight on resonant configurations, such that a photon-scattering event immediately afterwards has a high chance of scattering into the cross-polarized channel. In the presence of stochastic noise, however, a cross-polarized photon detection yields less information regarding the nuclear spin state, and therefore leads to a smaller increase in the likelihood of a second cross-polarized scattering event, which results in weaker bunching and thus a decreased $g_V^{(2)}(0)$. Second, the effect of intermediate photon-scattering events impeding the nuclear spin evolution, and thereby the decay of $g_V^{(2)}(\tau)$ via the quantum Zeno effect, is reduced. This reduced effect of a photon-scattering event on the nuclear spin evolution can be attributed to the decreased precision of the measurement performed on the nuclear spin system by the photon due to the averaging over stochastic shifts s. As can be seen in Fig. 4, however, neither of these effects alters the qualitative behavior of the correlation function. The decay of the intensity autocorrelation still changes from relatively fast and initially quadratic for low laser intensities, to slow and exponential for higher intensities. Observation of this quantum Zeno effect should therefore be possible if the broadening of the excitonic transition due to dephasing is significantly smaller than the broadening due to nuclear spins, such that a photon-scattering event still yields sufficient information of the nuclear spin state.

The time evolution of $g_V^{(2)}(\tau)$ in the above analysis is due to nuclear spin evolution alone, and the electron spin is assumed to remain in an eigenstate of the electron Zeeman Hamiltonian. In an isolated electron-nuclear spin system with a magnetic field $B_{\text{ext}} \gtrsim 100$ mT [39], this assumption is well justified, as electron spin relaxation by electron-nuclear spin flip flops is energetically forbidden. In practice, however, there are additional mechanisms that may lead to electron spin relaxation, which in turn will lead to an exponentially decaying intensity correlation function that cannot be stabilized by the nuclear quantum Zeno effect. For example, cotunneling of electrons in and out of the QD can lead to such electron spin relaxation, although we note that this mechanism can be strongly suppressed by tuning of the QD energy with an external electric field [41].

Another electron spin relaxation mechanism that might obscure the nuclear quantum Zeno dynamics is given by second-order electron-nuclear flip flops, which arise when an environment such as the phonon bath supplies or absorbs the flip-flop energy [40]. Such environment-assisted flip flops arise from the contact hyperfine Hamiltonian given by

$$H_{\text{hf}} = \sum_k A_k \left[S^z I_k^z + \frac{1}{2}(S^- I_k^+ + S^+ I_k^-) \right], \qquad (41)$$

when also in the presence of electron spin dephasing at a rate η, and lead to electron spin relaxation at a rate $\sim\eta\frac{\alpha^2}{\omega_e^2}$, where ω_e is the electronic Zeeman splitting as before and α gives the interaction energy with the unpolarized nuclear spin bath [21]. This relaxation mechanism is therefore suppressed by a strong external magnetic field and tuning of the temperature and electrostatic environment to minimize the dephasing rate; however, a theoretical estimate of η and α is beyond the scope of this work. Experimental measurement of the electron spin relaxation rate has confirmed the ω_e^{-2} suppression of relaxation by a magnetic field and achieved spin lifetimes of hundreds of μs at sub-Tesla magnetic fields [41], which is significantly slower than the resonance fluctuations that are important in this work [25]. Putting these observations together, we conclude that the nuclear quantum Zeno effect should therefore be observable for magnetic fields of $\sim$1 T, temperatures of $T = 4$ K, and using tuning of the charge state to maximize the electron spin lifetime.

VI. DISCUSSION AND CONCLUSION

In order to experimentally demonstrate the nuclear quantum Zeno effect predicted here, it would suffice to observe the characteristic change of the cross-polarized intensity autocorrelation function from quadratic to linear short-time behavior, as the intensity of the input laser light increases. The non-Markovian quadratic regime is the most challenging to observe since the intensity must be low enough that unobserved intermediate scattering events have vanishing probability, which in turn implies a long integration time of the experiment. Increasing the input laser intensity will introduce intermediate photon-scattering events that take place during a delay time τ of interest. If these photons can be detected, the polarization outcomes of these detection events need to be averaged over to calculate the degree of second-order coherence $g^{(2)}(\tau)$. If these events are lost and not detected, this averaging is automatically performed. Loss does not, therefore, invalidate the measurement as long as there is an estimate of the photon-scattering rate for a given intensity. Following Eq. (36), one expects a broadening as well as a change from quadratic to linear behavior of the intensity autocorrelation function with intensity, which is a second experimental feature of the nuclear quantum Zeno effect.

Our result paves the way for experimental demonstration of a nuclear spin effect in quantum dots, with implications for both fundamental theoretical investigations and photonic quantum computing. Importantly, our formulation of the quantum Zeno effect in terms of a two-time correlation function has the advantage that it is possible to observe the effect without initializing the system in a particular state. The intensity autocorrelation considers pairs of cross-polarized photon-detection events, the first of which effectively initializes the nuclear system in a state with increased likelihood of being close to resonance. The second photon count then probes how far the system has evolved away from this initial state, and intermediate photon counts disturb this evolution. This generalized description of a quantum Zeno effect in terms of imperfect measurements and two-time correlation functions likely applies to other experimentally accessible quantum systems. Another interesting theoretical aspect of the nuclear quantum Zeno process is the explicit connection between a measurement and the physical process of photon scattering. This connection shows that it is the coherence-destroying effect of measurements that impedes coherent evolution and gives rise to the quantum Zeno effect. The formulation of coherence reduction of photon scattering as a measurement is merely a convenient formalism, making it clear that a coherence-removing process that gives rise to a quantum Zeno effect does not need to be a measurement.

Beyond these implications, the nuclear quantum Zeno effect may be relevant to the experimental realization of a quantum-dot-based source of entangled photons. A weak laser could be used to stabilize the nuclear system in a state for which the electronic transition is close to resonance and where high phase shifts can be achieved. If a method was found to simultaneously keep the electron spin in a superposition, then the nuclear Zeno effect could be used to realize photonic states with useful entanglement properties, as proposed in [5], even in the presence of a nuclear spin environment.

ACKNOWLEDGMENTS

The authors thank John Rarity, Terry Rudolph, Sophia Economou, Ed Barnes, Will McCutcheon, and Gary Sinclair for interesting and useful discussions. T.N. acknowledges financial support from the People Programme (Marie Curie Actions) of the European Unions Seventh Framework Programme (Grant No. FP7/2007-2013) under REA Grant Agreement No. 317232. This project has received funding from the European Union's Horizon 2020 research and innovation programme under the Marie Skłodowska-Curie Grant Agreement No. 703193. This work was also funded by the Frontiers in Quantum Technologies programme and by the Engineering and Physical Sciences Research Council (Grants No. EP/M024156/1, No. EP/N003381/1, and No. EP/L024020/1).

[1] N. H. Lindner and T. Rudolph, Phys. Rev. Lett. **103**, 113602 (2009).
[2] S. E. Economou, N. Lindner, and T. Rudolph, Phys. Rev. Lett. **105**, 093601 (2010).
[3] I. Schwartz, D. Cogan, E. R. Schmidgall, Y. Don, L. Gantz, O. Kenneth, N. H. Lindner, and D. Gershoni, Science **354**, 434 (2016).
[4] C. Y. Hu, A. Young, J. L. O'Brien, W. J. Munro, and J. G. Rarity, Phys. Rev. B **78**, 085307 (2008).
[5] C. Y. Hu, W. J. Munro, and J. G. Rarity, Phys. Rev. B **78**, 125318 (2008).
[6] A. Pineiro-Orioli, D. P. S. McCutcheon, and T. Rudolph, Phys. Rev. B **88**, 035315 (2013).
[7] P. Lodahl, S. Mahmoodian, and S. Stobbe, Rev. Mod. Phys. **87**, 347 (2015).
[8] P. Lodahl, Quantum Sci. Technol. **3**, 013001 (2018).
[9] D. P. S. McCutcheon, N. H. Lindner, and T. Rudolph, Phys. Rev. Lett. **113**, 260503 (2014).
[10] A. V. Kuhlmann, J. H. Prechtel, J. Houel, A. Ludwig, D. Reuter, A. D. Wieck, and R. J. Warburton, Nat. Commun. **6**, 8204 (2015).
[11] R. Stockill, C. Le Gall, C. Matthiesen, L. Huthmacher, E. Clarke, M. Hugues, and M. Atatüre, Nat. Commun. **7**, 12745 (2016).
[12] G. Wuest, M. Munsch, F. Maier, A. V. Kuhlmann, A. Ludwig, A. D. Wieck, D. Loss, M. Poggio, and R. J. Warburton, Nat. Nanotech. **11**, 885 (2016).
[13] G. Ethier-Majcher, D. Gangloff, R. Stockill, E. Clarke, M. Hugues, C. Le Gall, and M. Atatüre, Phys. Rev. Lett. **119**, 130503 (2017).
[14] J. Greilich, M. Silva, O. Moussa, C. Ryan, M. Laforest, J. Baugh, D. G. Cory, and R. Laflamme, Science **317**, 1896 (2007).
[15] E. Barnes and S. E. Economou, Phys. Rev. Lett. **107**, 047601 (2011).
[16] K. H. Madsen, S. Ates, T. Lund-Hansen, A. Löffler, S. Reitzenstein, A. Forchel, and P. Lodahl, Phys. Rev. Lett. **106**, 233601 (2011).
[17] B. Urbaszek, X. Marie, T. Amand, O. Krebs, P. Voisin, P. Malentinsky, A. Högele, and A. Imamoglu, Rev. Mod. Phys. **85**, 79 (2013).
[18] S. E. Economou and E. Barnes, Phys. Rev. B **89**, 165301 (2014).
[19] M. Munsch, G. Wuest, A. V. Kuhlmann, F. Xue, A. Ludwig, D. Reuter, A. D. Wieck, M. Poggio, and R. J. Warburton, Nat. Nanotech. **9**, 671 (2014).
[20] J. H. Prechtel, A. V. Kuhlmann, J. Houel, A. Ludwig, S. R. Valentin, A. D. Wieck, and R. J. Warburton, Nat. Mater. **15**, 981 (2016).
[21] T. Nutz, E. Barnes, and S. E. Economou, Phys. Rev. B **99**, 035439 (2019).
[22] P. Androvitsaneas, A. B. Young, C. Schneider, S. Maier, M. Kamp, S. Hofling, S. Knauer, E. Harbord, C. Y. Hu, J. G. Rarity, and R. Oulton, Phys. Rev. B **93**, 241409(R) (2016).
[23] A. Auffèves-Garnier, C. Simon, J.-M. Gérard, and J.-P. Poizat, Phys. Rev. A **75**, 053823 (2007).
[24] A. Abragam, *The Principles of Nuclear Magnetism* (Clarendon, Oxford, 1961).
[25] P. Androvitsaneas, A. Young, J. Lennon, C. Schneider, S. Maier, J. Hinchliff, G. Atkinson, E. Harbord, M. Kamp, S. Hoefling, J. G. Rarity, and R. Oulton, ACS Photon. **6**, 429 (2019).
[26] B. Misra and E. C. G. Sudarshan, J. Math. Phys. **18**, 756 (1977).
[27] W. M. Itano, D. J. Heinzen, J. J. Bollinger, and D. J. Wineland, Phys. Rev. A **41**, 2295 (1990).
[28] E. Block and P. R. Berman, Phys. Rev. A **44**, 1466 (1991).
[29] P. Facchi, V. Gorini, G. Marmo, S. Pascazio, and E. Sudarshan, Phys. Lett. A **275**, 12 (2000).
[30] S. Pascazio, Open Syst. Inf. Dynamics **21**, 1440007 (2014).
[31] Y.-R. Zhang and H. Fan, Sci. Rep. **5**, 11509 (2015).
[32] C. N. Christensen, J. Iles-Smith, T. S. Petersen, J. Mørk, and D. P. S. McCutcheon, Phys. Rev. A **97**, 063807 (2018).
[33] C. W. Gardiner and M. J. Collett, Phys. Rev. A **31**, 3761 (1985).
[34] D. F. Walls and G. J. Milburn, *Quantum Optics*, 2nd ed. (Springer-Verlag, Berlin, 2008).
[35] D. Klauser, W. A. Coish, and D. Loss, Phys. Rev. B **78**, 205301 (2008).
[36] M. B. Plenio and P. L. Knight, Rev. Mod. Phys. **70**, 101 (1998).
[37] H. J. Carmichael, S. Singh, R. Vyas, and P. R. Rice, Phys. Rev. A **39**, 1200 (1989).
[38] A. Nazir and D. P. S. McCutcheon, J. Phys.: Condens. Matter **28**, 103002 (2016).
[39] Ł. Cywiński, W. M. Witzel, and S. Das Sarma, Phys. Rev. B **79**, 245314 (2009).
[40] C. Latta, A. Högele, Y. Zhao, A. N. Vamivakas, P. Maletinsky, M. Kroner, J. Dreiser, I. Carusotto, A. Badolato, D. Schuh, W. Wegscheider, M. Atature, and A. Imamoglu, Nat. Phys. **5**, 758 (2009).
[41] J. Dreiser, M. Atatüre, C. Galland, T. Müller, A. Badolato, and A. Imamoglu, Phys. Rev. B **77**, 075317 (2008).